Published in final edited form as:

J Immunol. 2017 June 01; 198(11): 4341–4351. doi:10.4049/jimmunol.1500106.

IL-1 receptor type 1 deficient mice demonstrate an impaired host immune response against cutaneous vaccinia virus infection

Tian Tian[*], **Michelle Qiushuang Jin**[†], **Krista Dubin**[‡], **Sandra L. King**[*], **Wolfram Hoetzenecker**[§], **George F. Murphy**[¶], **Chen Amy Chen**[‖], **Thomas S. Kupper**[*], and **Robert C. Fuhlbrigge**[#]

[*]Department of Dermatology, Brigham and Women's Hospital, Harvard Medical School, 77 Louis Pasteur Ave, Boston, MA 02115, USA [†]Stanford University, 450 Serra Mall, Stanford, CA 94305, USA [‡]Weill Cornell Medical College, 1300 York Avenue, New York, NY 10065, USA [§]Department of Dermatology, University Hospital of Zurich, Gloriastrasse 31, 8091 Zurich, Switzerland [¶]Department of Pathology, Brigham and Women's Hospital, Harvard Medical School, 221 Longwood Ave. Boston, MA 02115, USA [‖]Harvard Medical School, 25 Shattuck St. Boston, MA 02115, USA [#]Pediatric Rheumatology, University of Colorado- Denver, 13123 East 16th Avenue, Aurora, CO 80045

Abstract

The IL-1 superfamily of cytokines and receptors has been studied extensively. However, the specific roles of IL-1 elements in host immunity to cutaneous viral infection remain elusive. In this study, we applied vaccinia virus (VACV) by scarification to IL-1 receptor type 1 knockout mice (IL-1R1−/−) and found that these mice developed markedly larger lesions with higher viral genome copies in skin than wild-type (WT) mice. The phenotype of infected IL-1R1−/− mice was similar to eczema vaccinatum (EV), a severe side effect of VACV vaccination that may develop in humans with atopic dermatitis (AD). Interestingly, the impaired cutaneous response of IL-1R1−/− mice did not reflect a systemic immune deficiency, since immunized IL-1R1−/− mice survived subsequent lethal VACV intranasal challenge, or defects of T cell activation or T cell homing to the site of inoculation. Histologic evaluation revealed that VACV infection and replication after scarification were limited to the epidermal layer of WT mice, whereas lack of IL-1R1 permitted extension of VACV infection into dermal layers of the skin. We explored the etiology of this discrepancy and determined that IL-1R1−/− mice contained significantly more macrophages and monocyte-derived dendritic cells (mo-DC) in the dermis after VACV scarification. These cells were vulnerable to VACV infection and may augment the transmission of virus to adjacent skin, thus leading to larger skin lesions and satellite lesions in IL-1R1−/− mice. These results suggest

Direct correspondence to: Tian Tian, PhD, Department of Dermatology, Brigham and Women's Hospital, Harvard Medical School, 77 Louis Pasteur Ave, Boston, MA 02115, USA, Phone: 617-525-5573, FAX: 617-525-5571, ttian@partners.org; Robert Fuhlbrigge, MD PhD, Pediatric Rheumatology, University of Colorado- Denver, 13123 East 16th Avenue, Aurora, CO 80045, Phone: 720-777-6132, Fax: 720-777-7341, Robert.Fuhlbrigge@childrenscolorado.org.
All work for this manuscript was conducted in Boston, MA, USA

This work was supported by NIH/NIAID contract HHSN266200400030C (the NIH Atopic Dermatitis Vaccinia Network) to T.S. Kupper and R.C. Fuhlbrigge, NIH/NIAMS grant P30 AR42689 from the Harvard Skin Disease Research Center to T.Tian and a Research Grant from the Dermatology Foundation to T.Tian.

new therapeutic strategies for treatment of EV and inform assessment of risks in patients receiving IL-1 blocking antibodies for treatment of chronic inflammatory disorders.

Introduction

If complexity of a cytokine network is an index of its biological importance, very few cytokines can compare with IL-1. The IL-1 family of cytokines includes three ligands (IL-1α, IL-1β and the IL-1 receptor antagonist IL-1Ra) and two forms of IL-1 receptors (IL-1R1 and IL-1R2). IL-1α and IL-1β are synthesized by cells throughout the body including monocytes, macrophages, and neutrophils, as well as endothelial and epithelial cells. Both IL-1α and IL-1β signal through IL-1R1, whereas IL-1R2 is unable to transduce a signal and is generally considered to be a decoy receptor. IL-1Ra, which is produced in conjunction with IL-1α and IL-1β, also binds the IL-1R1 with high affinity but does not induce a signal, thus acting as an inhibitor of IL-1 mediated responses. After IL-1 binds to IL-1R1, an accessory protein (IL-1RAcP) joins with IL-1/IL-1R1 to form a signaling complex. This complex recruits intracellular adaptor molecules including myeloid differentiation factor 88 (MyD88), IL-1R associated kinase (IRAK) and TNF receptor-associated factor 6 (TRAF6), to activate a variety of signaling pathways including nuclear-factor κB (NF- κB), activator protein-1 (AP-1), c-Jun N-terminal kinase (JNK) and p38 mitogen-associated protein kinase (MAPK) (1).

Human skin is a complex immune environment in which all elements of the IL-1 axis are represented. IL-1 is not only an important regulator of host immune defense, but is also a potent contributor to inflammatory skin diseases, such as psoriasis and AD, which are associated with alterations in the balance of IL-1 proteins and receptors (2). The key role of IL-1 in host resistance to systemic viral infections such as intravenous adenovirus infection (3) and respiratory influenza virus infection (4) has been demonstrated in a variety of mouse models. However, the role of the IL-1 network in host immunity to cutaneous viral infection, particularly VACV skin infection, remains incompletely characterized.

Like other poxviruses, VACV encodes proteins that interfere with important components of host antiviral defense, including soluble cytokines, chemokine binding proteins and several cytokine and chemokine receptors (5). As IL-1 is a key initiator of the host defense against infection, linking the innate and acquired immune response systems, it is not surprising that VACV produces gene products that interfere with components of the IL-1/IL-1R1 pathway. As one example, VACV gene B15R encodes a glycoprotein that functions as a soluble IL-1R that binds IL-1β, but not IL-1α or IL-1Ra. Deletion of B15R from VACV has been shown to induce differential effects on infected mice depending on which inoculation route is used. For example, B15R-deficient VACV demonstrated increased virulence in intracranially infected mice and attenuated virulence in intranasally infected mice compared to wild type VACV (6). However, deletion of B15R from VACV did not alter pathogenesis in an intradermal (i.d.) injection model of VACV infection (7). These authors observed a similar phenotype with the B15R-deficient VACV and control VACV intradermal injection and did not provide a mechanism. The outcome of applying B15R-deficient VACV to mice by skin scarification has not been reported and is worth exploring in future studies. The use of

B15R-deficient VACV by skin scarification may produce different results than intradermal injection, based on previous studies from our laboratory which demonstrated significant differences in immune response between infections by intradermal injection versus skin scarification (8). Due to the similarity of IL-1R1 to Toll-like receptors (TLR), the conserved sequence in the cytosolic region of these proteins has been termed the Toll-IL-1 receptor (TIR) domain. The proteins activated during signaling by IL-1R1 also participate in signaling by other receptors with TIR domains (9). VACV proteins A46R and A52R target multiple TIR adaptors and contribute to virulence. Immune responses to VACV lacking A46R or A52R genes were attenuated in several models of infection in mice (10–12).

Mouse models have been utilized to study the role of MyD88, an essential downstream adaptor involved in IL-1R1 signaling. In VACV intradermal infection, which is a more natural route than systemic routes of infection such as intraperitoneal or intravenous injections, it was reported that MyD88 is required for induction of CD4 T cell and B cell responses and for control of virus replication at the inoculation site (13). MyD88 was also shown to be critical for CD8 T cell response after i.p. infection by VACV(14).

We investigated the roles of other IL-1 elements in VACV infection via skin scarification, the route used in humans to induce resistance to smallpox. In a previous study, we applied VACV by scarification to mice that over-expressed IL-1α in the epidermis (K14/IL-1α Tg mice) and found that the mice demonstrated enhanced innate and adaptive immune responses (15). In the present study, we applied VACV by scarification to IL-1R1−/− mice and found that these mice showed increased susceptibility, developing markedly larger lesions with higher viral genome copies in skin than WT mice. IL-1R1−/− mice also developed multiple satellite lesions in adjacent skin. This phenotype is very similar to eczema vaccinatum (EV) in humans, a severe side effect seen in atopic dermatitis (AD) patients following VACV scarification (16). Interestingly, the impaired immune response of IL-1R1−/− mice did not reflect a systemic immune deficiency, since IL-1R1−/− mice cleared virus from the skin and survived subsequent intranasal challenge with a lethal dose of VACV as well as immunized WT control animals. We further show that the impaired skin response of IL-1R1−/− mice following VACV scarification was not caused by defects of T cell activation or T cell skin homing. Further study revealed that while VACV infection and replication after scarification were limited to the epidermal layer of WT mice, lack of IL-1R1 permitted extension of productive VACV infection to deep dermal layers of the skin in IL-1R1−/− mice. We further demonstrate that IL-1R1−/− mice recruited significantly more macrophages and mo-DCs to the dermis after VACV scarification and that these cells were specifically vulnerable to VACV infection. We propose that the enhanced production of live virus in dermal macrophages and mo-DCs of IL-1R1−/− mice increases the transmission of virus to adjacent skin areas, thus leading to larger skin lesions and satellite lesions seen in IL-1R1−/− mice. This effect of impaired IL-1 signaling, leading to increased viral replication in recruited immune cells, may relate to the risk for EV seen in patients with AD and other inflammatory skin disorders.

Materials and Methods

Mice

IL-1R1 deficient mice and macrophage Fas-Induced Apoptosis (Mafia) transgenic mice were obtained from Jackson Laboratory (Bar Harbor, Maine) and bred in a biosafety level 1 (BL-1) facility at Harvard Medical School (HMS). Mafia mice were crossed with IL-1R1−/− mice to produce Mafia/IL-1R1−/− mice. C57BL/6J mice were purchased from Jackson Laboratory and used as WT controls. All mice were handled in accordance with guidelines set out by the Center for Animal Resources and Comparative Medicine at HMS.

Viruses, *in vivo* infection and viral load in tissues

Western Reserve vaccinia virus (WR-VACV, American Type Culture Collection, ATCC, Manassas, VA) and recombinant VACV expressing green fluorescent protein (rVACV-GFP, a kind gift from Dr. Bernard Moss, NIH) were expanded in HeLa cells and titered in CV-1 cells using standard procedures (17). Modified Vaccinia Ankara (MVA: ACAM3000MVA) was expanded and titered using DF-1 cells (ATCC) (17). Mice were inoculated with 5×10^6 plaque-forming units (pfu) of VACV or MVA by scarification at approximately 1cm from the base of the tail as described (17). Lesions were measured with a millimeter ruler every 2–4 days following scarification. For challenge experiments, mice were anesthetized with isoflurane and inoculated intranasally with 2×10^6 pfu of WR-VACV. Individual mice were weighed and checked for survival daily. Mice that lost more than 25% of original body weight were euthanized. Quantitative PCR was used to measure viral copy number in skin and various organs of infected mice as described (15). For analysis, inoculated skin was defined as the immediate area (0.5 cm in either direction) surrounding the inoculation site. 1cm length of skin adjacent to the inoculated skin towards the tip of the tail was defined as adjacent skin. Measurement with a caliper was performed to guarantee the same location in all mice.

Cell depletion

AP20187 ligand (Clotech) was used for *in vivo* macrophage depletion. It was dissolved in 4% (vol/vol) ethanol, 10% (vol/vol) polyethylene glycol 400, and 1.7% (vol/vol) Tween-20 and injected into Mafia mice (10 mg/kg) i.v. daily from day 0 to day 5 of VACV scarifications followed by AP20187 injections (1 mg/kg) every three days to maintain the depletion.

Measurement of vaccinia virus-specific antibody

Blood was drawn from infected mice at the indicated time points and VACV-specific antibody levels were determined as described (15).

Skin cell preparation and *in vitro* infection

Single cell suspensions from whole skin were prepared as described (8). Cells from epidermal skin and dermal skin were generated as described previously with some modification (18). Briefly, the skin samples were floated, dermis side down, on a solution containing 2.4 U/ml grade II dispase (Roche, Indianapolis, IN) for 40 min at 37°C.

Epidermis and dermis were gently teased away from each other and digested in HBSS skin digestion buffer which contains 25% FCS, 1mg/ml collagenase A, 40μg/ml DNAse I (Roche, Indianapolis, IN) and 5mM Ca^{2+} at 37°C for 30 min. The digested material was filtered through a 75 μm cell strainer to generate a single cell suspension. Cells were rinsed twice with PBS prior to infection in media containing rVACV-GFP at multiplicity of infection (MOI) ranging from 1 to 20. The cells were incubated for 6 h at 37 °C, 5% CO2 with gentle shaking every 15 min in the first 2 h to ensure an even distribution of media in the plates. GFP-positive VACV-infected cells were detected by flow cytometry.

Flow cytometry

Fluorochrome conjugated anti-mouse antibodies to NK1.1 (FITC), CD3 (PE), CD11b (FITC), Gr-1 (PE), F4/80 (PE), CD4 (FITC), and CD8 (PE) (all purchased from BD Biosciences) were used for cell surface staining. To detect VACV-specific $CD8^+$ T cells, single cell suspensions from inguinal lymph nodes (ILN), spleen and skin of immunized mice were stained with PE-conjugated B8R-pentamer (Proimmune, Oxford, U.K) as previously described (17). To detect T regulatory cells (Tregs), the cells were stained with antibodies to mouse FoxP3 (APC) as well as CD4 (FITC), CD25 (PE) and CD3 (PerCP) (eBioscience, San Diego, CA) according to the manufacture's protocol. For intracellular IFNγ staining, cells were first stimulated with 10 μM B8R $_{20–27}$ peptide at 37° C in 5% CO_2 in the presence of protein transport inhibitor cocktail (eBioscience) for 5h, and then stained with antibodies to mouse IFNγ (APC) in addition to CD8 (FITC) and CD3 (PerCP) from BD Biosciences. FITC conjugated IFNα, IFNβ from PBL Assay Science and IFNγ, TNFα from Biolegend were used to detect cytokine production by mo-DC/macrophages in inoculated skin, The single cells suspensions made from VACV infected skin were incubated with protein transport inhibitor cocktail for 4 hours prior to staining. The stained cells were acquired on a FACSCanto (BD Biosciences) flow cytometer and analyzed with FlowJo software (Version 6.4.7, Tree star, Ashland, OR). Lymphocytes were gated on CD19 negative cells for B8R-pentamer staining.

Cell sorting and Plaque assay to measure viral replication

Inoculated skin from mice scarified with rVACV-GFP (n=5 to 7 per group) was harvested and digested in HBSS skin digestion buffer at 37°C for 30 min. Cells were filtered, stained with PE-conjugated anti-CD45 mAb (BD Biosciences) and sorted (BD FACSAria) into GFP^+CD45^+ and GFP^-CD45^+subsets. Sorted cells were freeze-thawed 3 times, sonicated 3 times and the titer of vaccinia plaque forming unit (PFU) per sample was determined by standard plaque assay on CV-1 monolayers (19).

In vitro restimulation assay

Single cell suspensions were prepared from ILN and spleens of immunized mice and stimulated as previously described (17). Supernatants were collected at 40 h and cytokine concentrations in the supernatant were measured by ELISA (BD Biosciences, San Diego, CA).

Immunohistochemistry

Inoculated skin was harvested from three to four mice per group at each time point. To detect the presence of rVACV-GFP, skin was preserved in formalin, embedded in paraffin, sectioned, and stained with anti-GFP antibody (Clone JL-8; Clontech, Palo Alto, CA) as previously described (8). To detect F4/80 or late viral antigen B5R expression, skin samples were fixed in formalin, embedded in paraffin, sectioned (10 μm) and treated with 1× Target Retrieval Solution (Dako Cytomation). Sections were incubated with purified rat anti-mouse F4/80 antibody (AbD Serotec, Raleigh, NC, USA) or rat MAb19C2, (kind gifts from Bernard Moss, National Institutes of Health), followed by anti-rat horseradish peroxidase-conjugated antibody (Envision detection kit, DAKO). Images were obtained with a Nikon E600 microscope and a Nikon EDX-35 digital camera.

Statistics

The significance of observed differences between indicated groups was assessed by an unpaired Student's *t* test. Tests were 2-tailed with a confidence interval of 95%. *P* values < 0.05 were considered significant. Statistical analyses were performed with Prism software (v4.0, Graphpad Software, Inc., La Jolla, CA).

Results

1. IL-1R1 deficient mice developed larger skin lesions with higher viral counts compared to WT mice following VACV scarification

IL-1R1−/− mice and WT mice were scarified with 5×10^6 pfu of WR-VACV at the base of the tail and monitored for the development of pox lesions every 2–4 days. IL-1R1−/− mice started to exhibit larger skin lesions than WT mice seven days after VACV scarification and developed multiple satellite lesions at approximately day 10. Both IL-1R1−/− and WT mice ultimately survived VACV inoculation and skin lesions resolved three to four weeks after scarification (Figure 1A and 1B, left). To investigate whether the larger skin and satellite lesions were associated with virus replication and dissemination, we measured the viral copy number in inoculated tail skin and skin adjacent to the pox lesion using PCR to quantify VACV genome copies per μg DNA in the skin (20–22). As illustrated in Figure 1C, IL-1R1−/− mice possessed 10-fold more VACV copies in inoculated skin than WT mice at 3 days following scarification and comparable viral copies at later time points. The viral load difference between WT and IL-1R1−/− mice was even more dramatic in skin distal to the scarification site. IL-1R1−/− mice contained at least 100-fold more viral genome copies in skin adjacent to the site of VACV inoculation at day 3 than WT mice and 10-fold more viral genome copies at day 6. At day 10, viral copies could not be detected in adjacent skin in 50% of WT mice while 100% of IL-1R1−/− mice contained significant numbers of viral genome copies in adjacent skin. Thus, it appeared that IL-1R1−/− mice have a defect in controlling local VACV replication and dissemination that contributed to the formation of larger and more numerous skin lesions. Both IL-1 R1−/− and WT mice showed negligible weight loss on day 2 post-infection and then gained weight thereafter (Figure 1B, right), indicating neither strain experienced severe systemic effects. We also investigated whether the impaired cutaneous response of IL-1R1−/− mice to VACV scarification reflected a globally compromised immune response or a skin-specific immune dysfunction by

measuring viral genome copies present in peripheral organs. The amount of viral DNA in ILN, spleen, lung and liver was comparable between IL-1R1−/− and WT mice at all time points measured up to two weeks post scarification (Figure 1D). Although VACV preferentially replicates and accumulates in the ovaries after intraperitoneal infection (i.p.) (23), viral DNA cannot be detected in the ovaries of WT mice after skin scarification (s.s.) and appeared only sporadically in the ovaries of IL-1R1−/− mice (Supplementary Figure 1). These results indicate that the impaired host response of IL-1R1−/− mice to VACV scarification appeared to be restricted to skin.

2. IL-1R1−/− mice demonstrated functional T cell activation and antibody response following VACV scarification

Antigen-specific T cell proliferation and antibody production are presumed to be critical components of the immune response to primary viral infection. To understand the role of these mechanisms in the observed response to VACV scarification, we measured VACV-specific Ab and T cell cytokine production in IL-1R1−/− and WT mice following VACV scarification. IL-1R1−/− mice produced modestly higher titers of VACV-specific IgG and IgG2a in comparison with WT mice, indicating a Th1 response bias. The level of VACV-specific IgG1 was similar between IL-1R1 deficient and WT strains, demonstrating that there was no difference in Th2 response (Supplementary Figure 2A). Eight weeks after VACV scarification, we challenged IL-1R1−/− and WT mice with a lethal dose of WR-VACV by intranasal inoculation to confirm the establishment of systemic immunity. All of the immunized IL-1R1−/− and WT mice survived intranasal viral challenge, while naïve, unimmunized IL-1R1−/− and WT control mice both lost body weight at the same rate and died within one week after intranasal challenge (Supplementary Figure 2B). Together these results show that both IL-1R1−/− mice and WT mice are able to achieve fully functional systemic immunity to VACV following skin scarification.

In order to assess the T cell immune response in scarified mice, we used B8R-pentamer staining to enumerate VACV-specific $CD8^+$ T cells. We found that IL-1R1−/− mice possessed similar numbers of VACV-specific $CD8^+$ T cells in both spleen and ILN compared to WT mice at 7 days after VACV scarification (Figure 2A). VACV-specific cytokine production was assessed in *in vitro* restimulation assays utilizing cells from spleen or ILN. $CD8^+$ T cells from both spleen and ILN of IL-1R1−/− mice and WT mice produced comparable amounts of IFNγ following VACV-peptide stimulation, as measured by intracellular cytokine staining (ICC) (Figure 2B). Consistent with the results of ICC, spleen and ILN cells from IL-1R1−/− mice produced similar levels of VACV- specific IFNγ compared to WT mice 7 days after scarification. Trace amounts of IL-4 and IL-10 were also produced by spleen and ILN cells from both strains of mice (Figure 2 C).

To address the possibility that an attenuated T cell response could be masked by greater antigen levels in IL-1R1−/− mice due to higher virus counts in VACV infected skin, we scarified mice with MVA, a strain of VACV that does not replicate in mammalian cells. At 7 days after MVA scarification, IL-1R1−/− mice demonstrated a functional T cell response and produced similar amounts of IFNγ, IL-4 and IL-10 as WT mice (Figure 2D). Collectively, these data indicated that the impaired cutaneous response of IL-1R1−/− mice

following VACV scarification was not caused by a defect of T cell activation or additional antigen due to virus replication.

3. T cell homing to VACV- inoculated skin was not impaired in IL-1R1 deficient mice

To assess whether the impaired cutaneous response of IL-1R1−/− mice might indicate a defect in T cell homing to skin following VACV scarification, we performed flow cytometry studies on T cells recovered from inoculated skin of VACV-scarified IL-1R1−/− mice and WT mice seven days post scarification. Both IL-1R1−/− and WT mice displayed substantial numbers of $CD8^+$ T cells in inoculated skin (WT: 66.7% ± 1.25; IL-1R1−/−: 63% ± 2.23, $P > 0.05$) with a similar fraction of B8R-pentamer staining cells within the $CD8^+$ T cell subpopulation of each strain (WT: 14.1% ± 1.5; IL-1R1−/−: 15.7% ± 1.3, $P > 0.05$). Similar percentages of $CD4^+$ $FoxP3^+$ regulatory T cells in WT and IL-1 R1−/− mice (WT: 1.09% ± 0.05; IL-1R1−/−: 0.93 % ± 0.14, $P > 0.05$) excluded the possibility that the impaired cutaneous response in IL-1R1−/− mice was caused by enhanced recruitment of regulatory T cells to the site of infection. Furthermore, substantial IFNγ production in response to VACV peptide stimulation was observed in $CD8^+$ T cells isolated from inoculated skin (Figure 3). These results suggested that general T cell homing and VACV-specific $CD8^+$ T cell recruitment to skin were operational in IL-1R1−/− mice following VACV scarification and that the functions of VACV-specific $CD8^+$ T cells in the inoculated skin were not defective or suppressed.

4. Lack of IL-1R1 facilitated VACV infection and replication in the dermis *in vivo*

The observation that IL-1R1−/− mice demonstrated enhanced susceptibility to VACV cutaneous infection without evidence of defects in adaptive immune system prompted us to examine the innate immune response in the skin following scarification. For these studies, we used rVACV-GFP for scarification and the infection of skin cells was monitored by immunostaining for GFP. On day 3 following scarification, VACV infection was largely restricted to the epidermis of WT mice, while IL-1R1−/− mice demonstrated disseminated VACV infection involving both dermal cells and epidermal cells (Figure 4A). Since the expression of GFP in rVACV-GFP is driven by the P7.5 early-later promoter, this staining does not address whether the infection has the potential to produce progeny virus (24). To distinguish productive infection from abortive infection, we also measured the expression of the late viral protein B5R in VACV scarified skin (19). B5R positive cells were found in the epidermis of both WT and IL-1R1−/− mice, but only IL-1R1−/− mice demonstrated significant numbers of B5R positive cells in the dermis, suggesting productive infection of these cell (Supplementary Figure 3). We separated epidermal skin from dermal skin at serial time points following VACV scarification and measured viral genome copies in inoculated skin and adjacent skin (Figure 4B). The number of viral copies per μg DNA seen in inoculated epidermis from WT mice was consistent with that in full thickness skin (Figure 1C). IL-1R1−/− mice, in contrast, showed 10-fold higher levels of viral genome copies per μg DNA in the epidermal skin at day 4 compared to WT mice, and slightly more at day 6. The difference of viral load in the epidermis was even more pronounced in adjacent skin, with IL-1R1−/− mice showing 30-fold more viral copies per μg DNA than WT mice at day 4 and day 6. Interestingly, VACV DNA could not be detected in the inoculated or adjacent dermis of WT mice at any time point. Although significant VACV DNA was detected in

dermis at the inoculation site of IL- 1R1−/− mice on day 4 post-scarification, it was cleared by day 6 and absent in adjacent skin. In summary, VACV infection and replication were limited to the epidermal layer in WT mice, whereas deficiency of IL-1R1 permitted VACV infection with both early and late gene expression in the dermal layer and extension of viral infection to skin cells distant from the inoculation site.

5. IL-1R1 deficient mice show enhanced recruitment of macrophage-like cells to the dermis of VACV scarified mice

Skin contains both intrinsic stromal cells (primarily keratinocytes and fibroblasts) and bone marrow (BM)-derived hematopoietic cells. To investigate which cells were susceptible to VACV infection in IL-1R1 deficient mice, we cultured primary epidermal and dermal cells from naïve WT and IL-1R1−/− mice and infected them with GFP-VACV *in vitro*. Infection was monitored by the expression of GFP using flow cytometry. CD45 staining was used to differentiate hematopoietic cells ($CD45^+$) from skin stromal cells ($CD45^-$). We found that both epidermal and dermal stromal cells and hematopoietic cells from IL-1R1−/− mice and WT mice were equally susceptible to infection by VACV *in vitro*, with the number of infected cells increasing in proportion to the multiplicity of infection (MOI) (Figure 5A).

We next investigated the phenotype and kinetics of cells recruited to VACV- scarified skin. We collected epidermal and dermal cells from IL-1R1−/− and WT mice at different time points after VACV scarification and measured the percentage of NK cells, neutrophils, macrophages and $CD8^+$ T cells in the infected skin. VACV-scarified IL-1R1−/− and WT mice initially had very few NK cells ($CD3^-NK1.1^+$) present in skin. The proportion of NK cells in the skin increased at day 2 after VACV infection and peaked at day 4, with the majority of NK cells found in the dermis. There was no significant difference in percentage of NK cells between IL-1R1−/− and WT mice. Naïve IL-1R1−/− and WT mice had few neutrophils ($CD11b^+Gr\text{-}1^+$) in the epidermis or dermis. The proportion of neutrophils increased after VACV scarification, with two-fold more neutrophils in IL-1R1−/− dermis than WT dermis at day 4. The difference in the presence of dermal macrophages ($CD11b^+F4/80^+$) between IL-1R1−/− and WT mice was also striking. IL-1R1−/− mice contained two fold more macrophages in dermis at both day 2 and day 4 as compared to WT mice. In contrast to innate effector cells, the infiltration of $CD8^+$ T cells to the skin did not appear until day 4 and was more pronounced in the epidermis of both strains and was not significantly different in IL-1R1−/− mice than in WT mice (Figure 5B).

We examined the morphology of VACV-infected GFP-positive cells in the dermis of IL-1R1−/− mice 3 days after scarification and found that these cells were dendritic in character. The areas of GFP-staining closely corresponded to the distribution of F4/80-positive macrophage lineage cells. In contrast, very few F4/80-positive dendritic macrophages were detected in the dermis of WT mice (Figure 5C). FACS analysis was used to quantify VACV-infected cells and showed that IL-1R1−/− mice contained approximately two-fold more infected (GFP^+ $CD45^+$) leukocytes than WT mice (WT: 6.44%, IL-1R1−/−: 13%) at day 3 after VACV scarification. The majority of $CD45^+GFP^+$ cells were $CD11b^+CD207^-$ (> 95%), which indicates they are not Langerhans cells. Based on CD64 (high-affinity IgG receptor Fcγ R1) and Ly6C expression, these cells are a mixture of

monocyte-derived DCs (mo-DC, CD64 ^{high} Ly6C $^{low\ to\ high}$) and macrophages (CD64^{high} Ly6C^{low}) (Figure 5D) (25). Type 1 interferons (IFNα and IFNβ) and Th1 cytokines such as IFNγ and TNFα have been found to play essential roles in controlling vaccinia virus infection (19, 26). Therefore, we measured production of these cytokines by CD11b^{+}CD207^{-} CD64 ^{high} cells directly isolated from VACV inoculated skin without additional stimulation. We found that CD11b^{+}CD207^{-} CD64 ^{high} cells from WT mice produced more IFNα, IFNβ, IFNγ and TNFα compared with those from IL-1R1−/− mice. (Figure 5 E). The lower levels of these anti-viral cytokines might make the macrophages of IL-1R1−/− mice more susceptible to VACV infection. In fact, we demonstrated that these IL-1R1−/− cells were infected and able to generate new virus progeny by day 5 after scarification. We sorted CD45^{+}GFP^{+} cells from infected skin after VACV scarification and performed plaque assays. At day 3, similar virus levels were observed for WT and IL-1R1−/− mice (9,900 ± 458.3 pfu of virus/10^4 GFP^{+} leukocytes, WT vs 9400±655.7 pfu of virus/10^4 GFP^{+} leukocytes, IL-1R1−/−.). At day 5, the majority of infected leukocytes (≈80%) are still CD11b^{+}CD207^{-} CD64 ^{high}, a phenotype indicative of mo-DCs or macrophages. CD45^{+}GFP^{+} cells from IL-1R1−/mice produced significantly more virions per cell compared with WT mice (23,400±1587 pfu/10^4 GFP^{+} leukocytes, WT vs 85,500 ± 8679 pfu/10^4 GFP^{+} leukocytes, IL-1R1−/−) (Figure 5F), indicating that only IL-1R1−/− cells were productively infected at this time. In contrast, virus was never recovered from the GFP-negative leukocytes in the same inoculated skin samples. Together, these data indicate that IL-1R1−/− mice recruited significant amounts of mo-DCs/macrophages to inoculated skin after VACV scarification and that these cells produced less anti-viral cytokines and were more susceptible to VACV infection compared to WT mice.

6. Conditional macrophage ablation reduced viral genome copies in VACV- scarified skin of Mafia/IL-1R1−/− mice

Since IL-1R1−/− mice contained significantly more macrophages in inoculated skin after VACV scarification and these cells were vulnerable to VACV infection, we propose that this response aids in the transmission of virus to surrounding skin cells, thus leading to the higher viral load in the adjacent skin. To prove this hypothesis, we crossed IL-1R1−/− mice with Mafia transgenic mice possessing an inducible Fas suicide/apoptotic system as well as GFP driven by the mouse colony stimulating factor 1 receptor promoter. Administration of the dimerizing reagent AP20187 was shown to induce apoptosis of GFP $^{+}$ monocytes, macrophages and dendritic cells in Mafia mice. In this model, neutrophils express low levels of GFP and will not be depleted by AP20187 treatment (27, 28). In our studies, repeated injections of AP20187 depleted > 90% GFP^{+}CD45^{+} leukocytes in inoculated skin of both Mafia and Mafia/IL-1R1−/− mice after VACV scarification (Figure 6A, left). Without AP20187 treatment, Mafia/IL-1R1−/− mice contained significantly more CD11b^{+}CD207^{-} CD64 ^{high} mo-DC/macrophages in VACV scarified skin compared to Mafia mice. After AP20187 treatment, more than 90% of mo-DC/macrophages were depleted in both mouse strains. (Figure 6A, right). We harvested inoculated skin and adjacent skin 3 days and 6 days after VACV scarification and measured viral genome copies. For Mafia mice, AP20187 treatment did not affect viral load at day 3 although significantly more viral genome copies were measured in inoculated skin at day 6. In contrast, AP20187- treated Mafia/IL-1R1−/− mice possessed 10-fold fewer VACV copies in inoculated skin on day 3 and day 6 compared

to mock-treated Mafia/IL-1R1−/− mice. The difference in viral load was more dramatic in adjacent skin where AP20187-treated Mafia/IL-1R1−/− mice contained 100-fold fewer VACV copies at both times points compared to mock-treated Mafia/IL-1R1−/− mice (Figure 6 B). We therefore conclude that depletion of mo-DCs/macrophages can reduce viral load in Mafia/IL-1R1−/− mice after VACV scarification and confirmed that macrophages/mo-DCs are involved in dissemination of VACV in scarified Mafia/IL-1R1−/− mice.

Discussion

IL-1 is a potent inflammatory cytokine that links innate and adaptive immune response mechanisms. In a previous study, we found that transgenic mice that overexpressed IL-1α in the epidermis (K14/IL-1α) displayed enhanced innate and adaptive immune responses to VACV inoculation by skin scarification (15). In the present study, we found that mice lacking IL-1R1 showed an impaired cutaneous immune response to VACV infection by skin scarification, resulting in an enhanced primary lesion size and the development of satellite lesions. Interestingly, IL-1R1−/− mice were able to generate an effective VACV-specific antibody response, as well as both $CD8^+$ effector and $FOXP3^+$ regulatory T cells responses, following VACV scarification. Further studies revealed that the observed response in IL-1R1−/− mice correlated with the disruption of innate immune response mechanisms. VACV infection was found to be restricted to the epidermal layer in WT mice inoculated by skin scarification, while inoculation of IL-1R1 −/− mice resulted in the infection of both epidermal and dermal layers of the skin and enhanced accumulation of VACV infected dermal macrophages and monocyte-derived DCs in the dermis. These macrophage lineage cells produced live virus and were thus able to support increased VACV replication and dissemination to skin cells distant from the inoculation site. Depletion of the mo-DC and macrophages from Mafia/IL-1R1−/− mice significantly reduced viral genome copies in VACV scarified skin at early time points.

IL-1R1−/− mice have been studied in a variety of bacterial and viral infectious disease models, but the precise role of IL-1R1 in the balance between innate and adaptive immune systems remains incompletely characterized. In bacterial infection models, inhibition of the innate immune response is the predominant effect seen from disruption of the IL-1 signaling pathway (29, 30). In contrast, viral infection models have shown a more profound influence of IL-1 signaling in the adaptive immune response. For example, IL-1R1−/− mice were more susceptible to respiratory influenza virus infection (influenza virus strain PR8) and showed both a markedly reduced IgM response and impaired recruitment of $CD4^+$ T cells to the site of infection (4). IL-1R1−/− mice infected with lymphocytic choriomeningitis virus (LCMV) also exhibited reduced expansion and proliferation of virus-specific $CD8^+$ T cells and an inability to clear LCMV compared to WT control mice (31).

Since the immune response to vaccinia virus is of high interest, due in part to its use for immunization against smallpox, a number of studies have been performed addressing the influence of innate and adaptive immune mechanisms on the containment of virus and the development of systemic immunity. In an intradermal VACV infection model, in which mice are inoculated with virus in the ear skin, the area was infiltrated first by macrophages, followed by granulocytes and then by lymphocytes (32, 33). Effective vaccination against

smallpox in humans has historically been achieved by inoculation of live VACV into the skin via scarification. In an ear scarification model, VACV was shown to infect both keratinocytes and migratory monocytes, which were then eliminated by infiltrating $CD8^+$ T cells (34). The positive influence of IL-1 on innate and adaptive immune responses to VACV scarification was shown in our previous report using K14/IL-1α Tg mice that over express IL-1α in the epidermis (15). These mice demonstrated enhanced VACV-specific T cell proliferation and VACV- specific antibody production in response to scarification, as compared to WT mice, along with increased recruitment of T cells and dendritic cells to the site of inoculation and more rapid clearance of virus from the skin by innate immune cells. In the present study using IL-1R1−/− mice, we found that production of VACV-specific Ab after scarification was not altered, and that both T cell cytokine production and T cell homing to skin was unaffected in these mice. Our interpretation of these results is that the impaired cutaneous response to VACV scarification seen in IL-1R1−/− mice reflects an alteration in the innate immune response.

Although the larger lesion phenotype seen in IL-1R1 deficient mice is similar to the effect we reported previously in TNFR1−/− mice (17), the mechanism appears to be different. In the prior study, we showed that the skin stromal cells of TNFR1−/− mice could not upregulate CRAMP, an antimicrobial peptide that provides critical antiviral activity, in response to VACV infection and thus could not effectively control the early stages of viral proliferation and distribution (35). Contrary to our results in TNFR1 deficient mice, IL-1R1−/− mice show enhanced CRAMP expression relative to WT mice (data not shown).

Immunostaining of mouse skin inoculated with recombinant VACV by scarification showed that VACV infection and replication were limited to the epidermal layer in WT mice, yet extended deep into the dermal layer in IL-1R1−/− mice. While the dermis of WT mice had no detectable viral DNA at any point after VACV scarification, a significant number of viral genome copies appeared in the dermis of IL-1R1−/− mice at day 4 after VACV scarification. The localization of VACV in the dermis of IL-1R1−/− mice correlated with the presence and distribution of $F4/80^+$ macrophage-like cells, which could be productively infected with vaccina.

Macrophages have been shown to serve different functions in two models of VACV infection. In the VACV intradermal infection mouse model, macrophages can infiltrate the site of infection and directly inhibit the spread of the virus. Here VACV replication was completely confined to the ear skin until clodronate liposomes were used to deplete macrophages and replicating VACV was observed to disseminate to the ovaries (28). In primary human macrophages *in vitro*, the cells are permissive to VACV infection and can be a vehicle for VACV replication and dissemination. These macrophages can produce extracellular enveloped virions for long-range VACV dissemination and form virion-associated structures contributing to cell-cell spread (36). Although the co-expression of CD11b and F4/80 has been often been used to identify macrophage-lineage cells, macrophages cannot be accurately distinguished from conventional DCs ($CD11b^+$DC) and mo-DCs in skin. A combination of cell-surface markers has recently been described to differentiate these cell populations in healthy and inflamed skin (25). After excluding Langerhans cells (LCs) that are $CD11b^+$ $CD207^+$ by gating, the remaining $CD11b^+$ $CD207^-$

cells can be further subdivided into $CD11b^{+}$DCs ($CD64^{-}MerTK^{-}CCR2^{+}Ly6C^{-}$), monocytes ($CD64^{lo}MerTK^{-to\ lo}CCR2^{+}Ly6C^{high}$), mo-DCs ($CD64^{-to\ +}MerTK^{-\ to\ lo}$ $CCR2^{+}Ly6C^{\ lo\ to\ high}$) and macrophages ($CD64^{high}MerTK^{+}CCR2^{lo}Ly6C^{lo}$). Using this expanded panel of markers to characterize the macrophage-like cells in VACV-infected skin, we found that the infected leukocytes ($CD45^{+}GFP^{+}$) cells were almost exclusively $CD11b^{+}CD207^{-}$ 3 days after VACV scarification in both WT and IL-1R1−/− mice. The pattern of CD64 and Ly6C expression suggested it is a mixed population of both mo-DCs and macrophages. In IL-1R1−/− mice, the enhanced infiltration of mo-DCs/macrophages and their susceptibility to infection may lead to increased dissemination of VACV to adjacent skin and cause the larger skin lesions and satellite lesions seen in IL-1R1−/− mice, but not WT mice. Depletion of mo-DCs/macrophages with AP20187 in Mafia/IL-1R1−/− mice dramatically reduced viral genome copies in VACV-scarified skin at early stage compared to untreated control Mafia/IL-1R1−/− mice. Multiple satellite lesions were found on the control Mafia/IL-1R1−/− mice 10 days after VACV scarification while very few AP20187-treated Mafia/IL-1R1−/− developed satellite lesions sporadically (data not shown). These data indicate that mo-DCs and macrophages play important roles in cutaneous VACV infection. The observation that T cell responses are unaffected in IL-1R1−/− mice allows for eventual effective control of viral replication and the development of protective immunity. Infection of skin leukocytes after VACV scarification has been reported previously, but the phenotype of infected leukocytes was somewhat different than in the present study. The previous study indicated that the majority of VACV infected leukocytes were inflammatory monocytes, along with minor populations of DCs, $Ly6G^{+}$ neutrophils and $Ly6G^{+}$monocytes (34). The discrepancy between these two studies may reflect the different location of skin scarification (tail vs ear) and different combinations of surface markers used for flow cytometry.

As both IL-1α and IL-1β use IL-1R1 to mediate their biological activities, the impaired cutaneous response to VACV in IL-1R1−/− mice may reflect a requirement for either IL-1α or IL-1β, or both, for optimal anti-VACV immune response. Production of IL-1α and IL-1β is largely segregated in the different anatomic layers in skin. IL-1α is constitutively expressed by epithelial cells, while IL-1β is more abundant in hematopoietic cells (1, 37, 38). To investigate the role of IL-1α versus IL-1β, we performed preliminary studies in which mice deficient in IL-1α or IL-1β were inoculated with VACV by scarification. In these studies we found that both IL-1α−/− and IL-1β−/− mice developed larger skin lesions and higher virus counts in adjacent skin compared to WT controls (Supplementary Figure 4). The skin lesions observed in IL-1α−/− mice were more dramatic than those of IL-1β−/− mice and IL-1α−/− mice exhibited more satellite lesions. This phenotypic difference suggests that these two IL-1R1 ligands may have distinct roles in the regulation of the skin immune response to VACV scarification. Further studies are needed to clarify the influence of IL-1α and IL-1β in restricting VACV replication in mo-DCs/macrophages *in vivo*.

In conclusion, elements of the IL-1 network including IL-1α, IL-1β and IL-1R1 are essential for the optimal host response to VACV cutaneous infection. Our study may lead to new therapeutic strategies for treatment of EV and contribute to risk assessment for viral infections in patients receiving IL-1 blocking antibodies for treatment of chronic inflammatory disorders.

Supplementary Material

Refer to Web version on PubMed Central for supplementary material.

Acknowledgments

We thank Dr. Niro Anandasabapathy for helpful discussions and for critically reviewing the manuscript.

Nonstandard abbreviations used

AD	atopic dermatitis
EV	eczema vaccinatum
IL-1R	IL-1 receptor
IL-1Ra	IL-1 receptor antagonist
ILN	inguinal lymph node
LCMV	lymphocytic choriomeningitis virus
Mafia	macrophage fas-induced apoptosis
MVA	Modified Vaccinia Ankara
TIR	Toll-IL-1 receptor
VACV	vaccinia virus
WR	Western Reserve strain
WT	wild-type,
mo-DC	monocyte-derived DC

References

1. Sims JE, Smith DE. The IL-1 family: regulators of immunity. Nature reviews. 2010; 10:89–102.
2. Murphy JE, Robert C, Kupper TS. Interleukin-1 and cutaneous inflammation: a crucial link between innate and acquired immunity. The Journal of investigative dermatology. 2000; 114:602–608. [PubMed: 10692124]
3. Shayakhmetov DM, Li ZY, Ni S, Lieber A. Interference with the IL-1-signaling pathway improves the toxicity profile of systemically applied adenovirus vectors. J Immunol. 2005; 174:7310–7319. [PubMed: 15905578]
4. Schmitz N, Kurrer M, Bachmann MF, Kopf M. Interleukin-1 is responsible for acute lung immunopathology but increases survival of respiratory influenza virus infection. Journal of virology. 2005; 79:6441–6448. [PubMed: 15858027]
5. Bahar MW, Graham SC, Chen RA, Cooray S, Smith GL, Stuart DI, Grimes JM. How vaccinia virus has evolved to subvert the host immune response. Journal of structural biology. 2011; 175:127–134. [PubMed: 21419849]
6. Alcami A, Smith GL. A soluble receptor for interleukin-1 beta encoded by vaccinia virus: a novel mechanism of virus modulation of the host response to infection. Cell. 1992; 71:153–167. [PubMed: 1394428]

7. Tscharke DC, Reading PC, Smith GL. Dermal infection with vaccinia virus reveals roles for virus proteins not seen using other inoculation routes. The Journal of general virology. 2002; 83:1977–1986. [PubMed: 12124461]

8. Liu L, Zhong Q, Tian T, Dubin K, Athale SK, Kupper TS. Epidermal injury and infection during poxvirus immunization is crucial for the generation of highly protective T cell-mediated immunity. Nature medicine. 2010; 16:224–227.

9. O'Neill LA. The interleukin-1 receptor/Toll-like receptor superfamily: 10 years of progress. Immunological reviews. 2008; 226:10–18. [PubMed: 19161412]

10. Bowie A, Kiss-Toth E, Symons JA, Smith GL, Dower SK, O'Neill LA. A46R and A52R from vaccinia virus are antagonists of host IL-1 and toll-like receptor signaling. Proceedings of the National Academy of Sciences of the United States of America. 2000; 97:10162–10167. [PubMed: 10920188]

11. Harte MT, Haga IR, Maloney G, Gray P, Reading PC, Bartlett NW, Smith GL, Bowie A, O'Neill LA. The poxvirus protein A52R targets Toll-like receptor signaling complexes to suppress host defense. The Journal of experimental medicine. 2003; 197:343–351. [PubMed: 12566418]

12. Stack J, Haga IR, Schroder M, Bartlett NW, Maloney G, Reading PC, Fitzgerald KA, Smith GL, Bowie AG. Vaccinia virus protein A46R targets multiple Toll-like-interleukin-1 receptor adaptors and contributes to virulence. The Journal of experimental medicine. 2005; 201:1007–1018. [PubMed: 15767367]

13. Davies ML, Sei JJ, Siciliano NA, Xu RH, Roscoe F, Sigal LJ, Eisenlohr LC, Norbury CC. MyD88-dependent immunity to a natural model of vaccinia virus infection does not involve Toll-like receptor 2. Journal of virology. 2014; 88:3557–3567. [PubMed: 24403581]

14. Zhao Y, De Trez C, Flynn R, Ware CF, Croft M, Salek-Ardakani S. The adaptor molecule MyD88 directly promotes CD8 T cell responses to vaccinia virus. J Immunol. 2009; 182:6278–6286. [PubMed: 19414781]

15. Tian T, Liu L, Freyschmidt EJ, Murphy GF, Kupper TS, Fuhlbrigge RC. Overexpression of IL-1alpha in skin differentially modulates the immune response to scarification with vaccinia virus. The Journal of investigative dermatology. 2009; 129:70–78. [PubMed: 18615110]

16. Engler RJ, Kenner J, Leung DY. Smallpox vaccination: Risk considerations for patients with atopic dermatitis. The Journal of allergy and clinical immunology. 2002; 110:357–365. [PubMed: 12209080]

17. Tian T, Dubin K, Jin Q, Qureshi A, King SL, Liu L, Jiang X, Murphy GF, Kupper TS, Fuhlbrigge RC. Disruption of TNF-alpha/TNFR1 function in resident skin cells impairs host immune response against cutaneous vaccinia virus infection. The Journal of investigative dermatology. 2012; 132:1425–1434. [PubMed: 22318381]

18. Deng L, Dai P, Parikh T, Cao H, Bhoj V, Sun Q, Chen Z, Merghoub T, Houghton A, Shuman S. Vaccinia virus subverts a mitochondrial antiviral signaling protein-dependent innate immune response in keratinocytes through its double-stranded RNA binding protein, E3. Journal of virology. 2008; 82:10735–10746. [PubMed: 18715932]

19. Liu L, Xu Z, Fuhlbrigge RC, Pena-Cruz V, Lieberman J, Kupper TS. Vaccinia virus induces strong immunoregulatory cytokine production in healthy human epidermal keratinocytes: a novel strategy for immune evasion. Journal of virology. 2005; 79:7363–7370. [PubMed: 15919891]

20. Freyschmidt EJ, Mathias CB, MacArthur DH, Laouar A, Narasimhaswamy M, Weih F, Oettgen HC. Skin inflammation in RelB(−/−) mice leads to defective immunity and impaired clearance of vaccinia virus. The Journal of allergy and clinical immunology. 2007; 119:671–679. [PubMed: 17336617]

21. Oyoshi MK, Elkhal A, Kumar L, Scott JE, Koduru S, He R, Leung DY, Howell MD, Oettgen HC, Murphy GF, Geha RS. Vaccinia virus inoculation in sites of allergic skin inflammation elicits a vigorous cutaneous IL-17 response. Proceedings of the National Academy of Sciences of the United States of America. 2009; 106:14954–14959. [PubMed: 19706451]

22. Freyschmidt EJ, Mathias CB, Diaz N, MacArthur DH, Laouar A, Manjunath N, Hofer MD, Wurbel MA, Campbell JJ, Chatila TA, Oettgen HC. Skin inflammation arising from cutaneous regulatory T cell deficiency leads to impaired viral immune responses. J Immunol. 2010; 185:1295–1302. [PubMed: 20548030]

23. Zhao Y, Adams YF, Croft M. Preferential replication of vaccinia virus in the ovaries is independent of immune regulation through IL-10 and TGF-beta. Viral immunology. 2011; 24:387–396. [PubMed: 21958373]
24. Earl PL, Americo JL, Moss B. Development and use of a vaccinia virus neutralization assay based on flow cytometric detection of green fluorescent protein. Journal of virology. 2003; 77:10684–10688. [PubMed: 12970455]
25. Tamoutounour S, Guilliams M, Montanana Sanchis F, Liu H, Terhorst D, Malosse C, Pollet E, Ardouin L, Luche H, Sanchez C, Dalod M, Malissen B, Henri S. Origins and functional specialization of macrophages and of conventional and monocyte-derived dendritic cells in mouse skin. Immunity. 2013; 39:925–938. [PubMed: 24184057]
26. Deonarain R, Alcami A, Alexiou M, Dallman MJ, Gewert DR, Porter AC. Impaired antiviral response and alpha/beta interferon induction in mice lacking beta interferon. Journal of virology. 2000; 74:3404–3409. [PubMed: 10708458]
27. Burnett SH, Kershen EJ, Zhang J, Zeng L, Straley SC, Kaplan AM, Cohen DA. Conditional macrophage ablation in transgenic mice expressing a Fas-based suicide gene. Journal of leukocyte biology. 2004; 75:612–623. [PubMed: 14726498]
28. Fischer MA, Davies ML, Reider IE, Heipertz EL, Epler MR, Sei JJ, Ingersoll MA, Rooijen NV, Randolph GJ, Norbury CC. CD11b(+), Ly6G(+) cells produce type I interferon and exhibit tissue protective properties following peripheral virus infection. PLoS pathogens. 2011; 7:e1002374. [PubMed: 22102816]
29. Deckert M, Virna S, Sakowicz-Burkiewicz M, Lutjen S, Soltek S, Bluethmann H, Schluter D. Interleukin-1 receptor type 1 is essential for control of cerebral but not systemic listeriosis. The American journal of pathology. 2007; 170:990–1002. [PubMed: 17322383]
30. Miller LS, O'Connell RM, Gutierrez MA, Pietras EM, Shahangian A, Gross CE, Thirumala A, Cheung AL, Cheng G, Modlin RL. MyD88 mediates neutrophil recruitment initiated by IL-1R but not TLR2 activation in immunity against Staphylococcus aureus. Immunity. 2006; 24:79–91. [PubMed: 16413925]
31. Joeckel LT, Wallich R, Metkar SS, Froelich CJ, Simon MM, Borner C. Interleukin-1R signaling is essential for induction of proapoptotic CD8 T cells, viral clearance, and pathology during lymphocytic choriomeningitis virus infection in mice. Journal of virology. 86:8713–8719.
32. Jacobs N, Chen RA, Gubser C, Najarro P, Smith GL. Intradermal immune response after infection with Vaccinia virus. The Journal of general virology. 2006; 87:1157–1161. [PubMed: 16603516]
33. Reading PC, Smith GL. A kinetic analysis of immune mediators in the lungs of mice infected with vaccinia virus and comparison with intradermal infection. The Journal of general virology. 2003; 84:1973–1983. [PubMed: 12867627]
34. Hickman HD, Reynoso GV, Ngudiankama BF, Rubin EJ, Magadan JG, Cush SS, Gibbs J, Molon B, Bronte V, Bennink JR, Yewdell JW. Anatomically restricted synergistic antiviral activities of innate and adaptive immune cells in the skin. Cell host & microbe. 2013; 13:155–168. [PubMed: 23414756]
35. Howell MD, Gallo RL, Boguniewicz M, Jones JF, Wong C, Streib JE, Leung DY. Cytokine milieu of atopic dermatitis skin subverts the innate immune response to vaccinia virus. Immunity. 2006; 24:341–348. [PubMed: 16546102]
36. Byrd D, Shepherd N, Lan J, Hu N, Amet T, Yang K, Desai M, Yu Q. Primary human macrophages serve as vehicles for vaccinia virus replication and dissemination. Journal of virology. 2014; 88:6819–6831. [PubMed: 24696488]
37. Arend WP, Palmer G, Gabay C. IL-1, IL-18, and IL-33 families of cytokines. Immunological reviews. 2008; 223:20–38. [PubMed: 18613828]
38. Dinarello CA. Immunological and inflammatory functions of the interleukin-1 family. Annual review of immunology. 2009; 27:519–550.

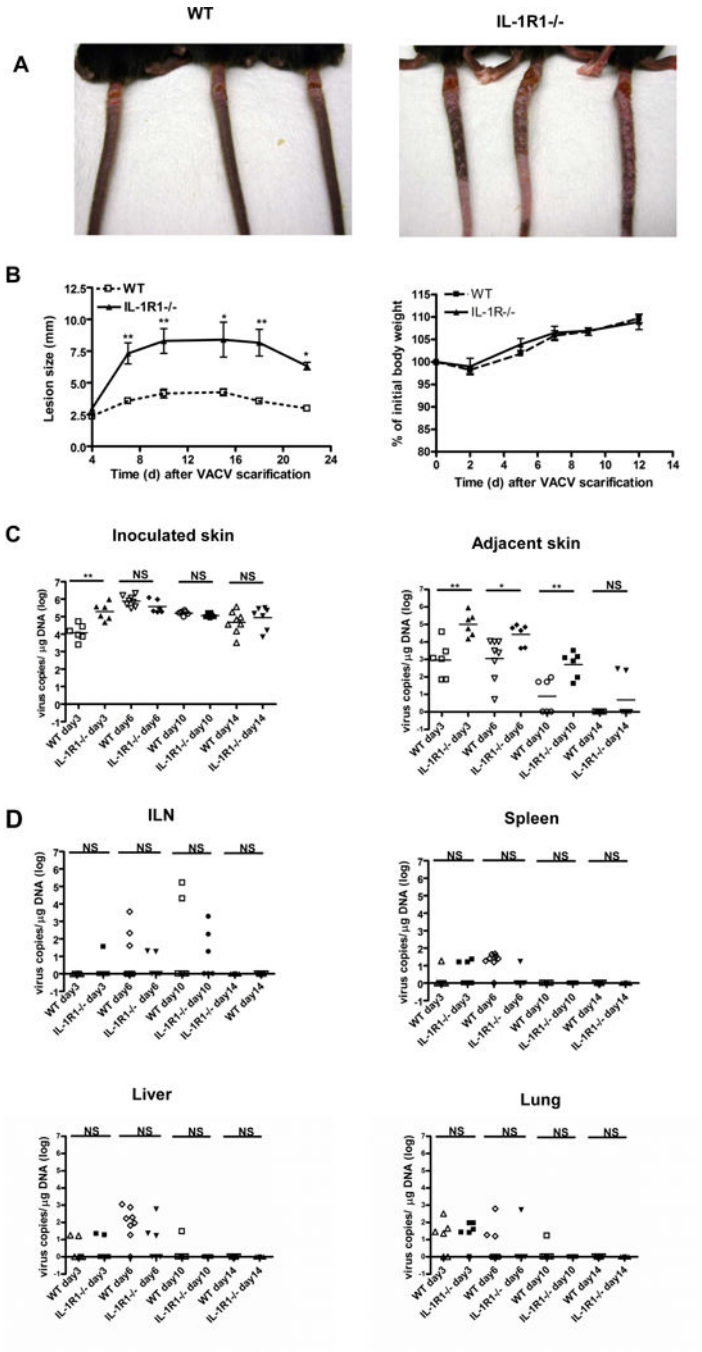

Figure 1. IL-1R1−/− mice developed markedly larger skin lesions with higher viral counts than WT mice following VACV scarification

5×10^6 pfu of WR-VACV was applied to the base of the tail by scarification for all studies. (A) Photographs were taken at day 11. (B) Skin lesions were measured and mice were weighed at indicated time points. (C) VACV copy number per μg DNA was determined by quantitative PCR in inoculated and adjacent skin following VACV scarification. (D) VACV copy number per μg DNA was determined by quantitative PCR in peripheral organs following VACV scarification. Error bars represent mean ± SEM. n = 5–8 per group. * $P < 0.05$, ** $P < 0.01$, *** $P < 0.001$, NS = not significant.

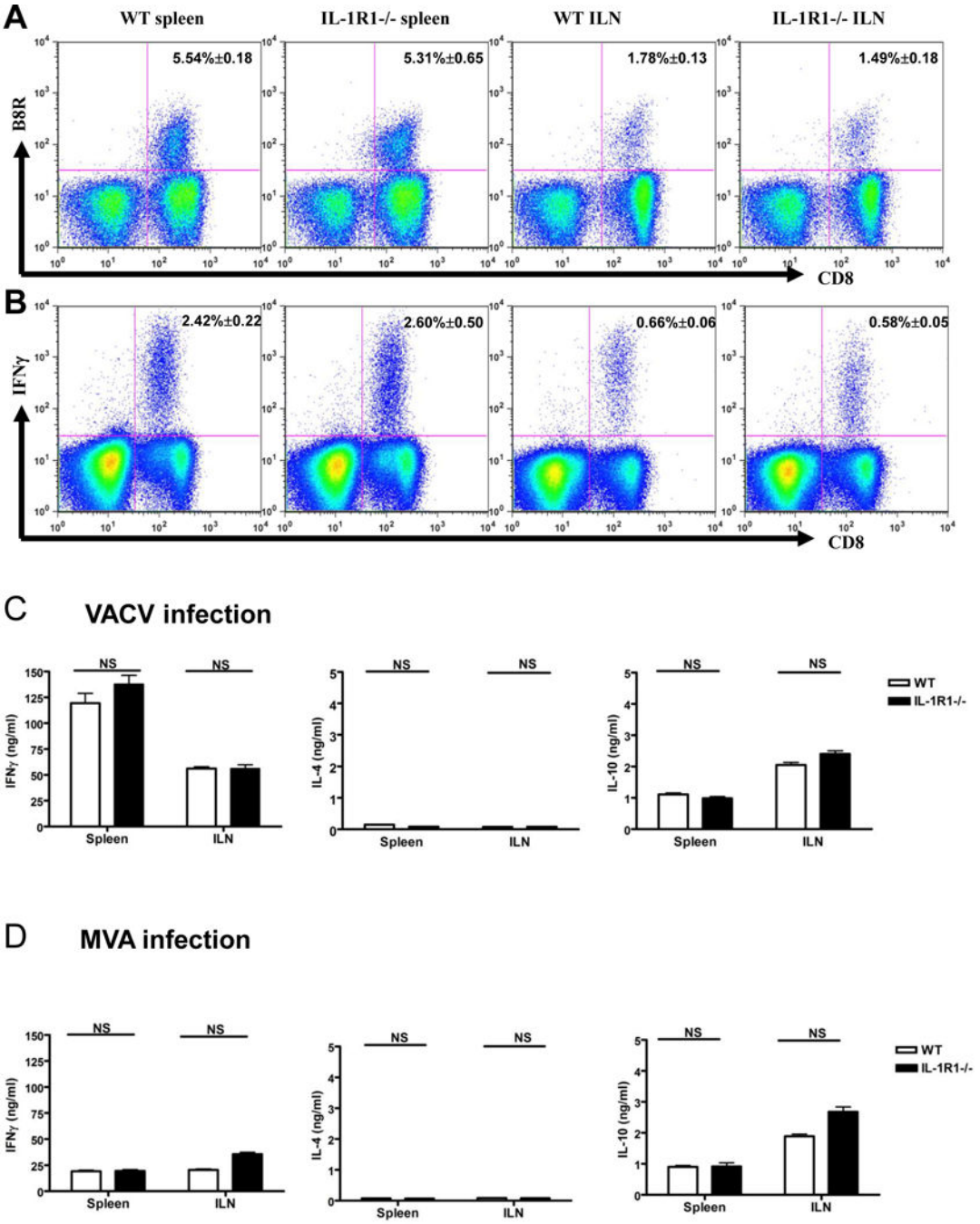

Figure 2. Type 1 T cell immune response was not altered by IL-1R1 deficiency

5×10^6 pfu of WR-VACV was applied to IL-1R1−/− and WT mice by scarification. At day 7, cells were harvested from spleens and ILNs for (A) B8R-pentamer staining to identify VACV-specific $CD8^+$ T cells and (B) Intracellular IFNγ staining following *in vitro* restimulation with VACV peptide $B8R_{20–27}$. Representative dot plots are shown with leukocytes gated using side and forward scatter. n=5 per group. 7 days after 5×10^6 pfu of VACV (C) or MVA (D) scarification. *In vitro* restimulation was used to detect VACV-specific IFNγ, IL-4 and IL-10 production from spleen and ILN cells. Error bars represent

mean ± SEM. n = 5–8 per group. * $P < 0.05$, ** $P < 0.01$, *** $P < 0.001$, NS = not significant.

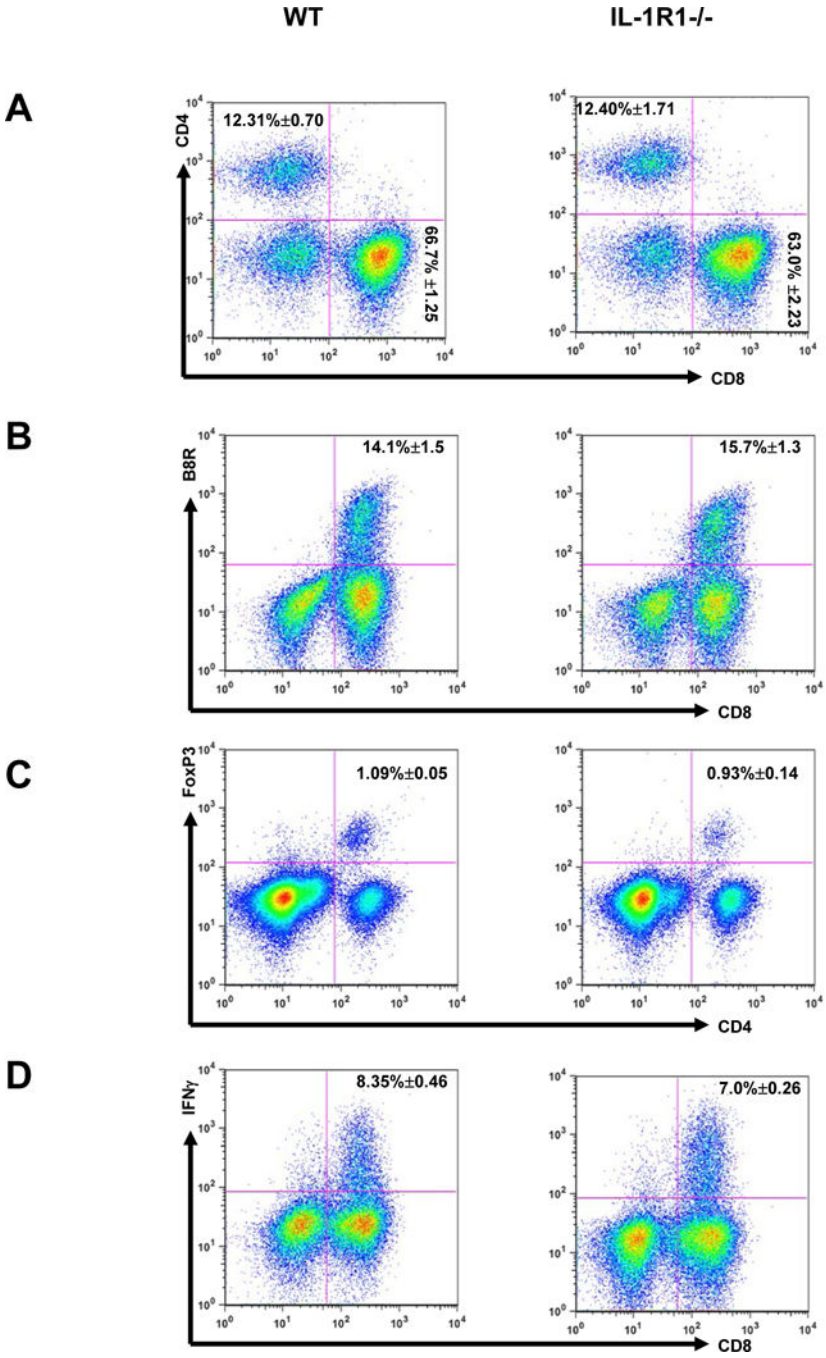

Figure 3. T cell homing to the VACV- inoculated skin did not depend on IL-1R1

5×10^6 pfu of WR-VACV was applied to IL-1R1−/− and WT mice by scarification. At day 7, (A) $CD4^+$ and $CD8^+$ T cells, (B) VACV-specific B8R-pentamer$^+CD8^+$ T cells and (C) $CD4^+$ $FoxP3^+$ regulatory T cells recruited to the inoculation site were measured using flow cytometry. (D) Skin cells were stimulated *in vitro* with VACV peptide $B8R_{20–27,}$ intracellular staining of IFNγ was performed with surface staining of CD8. Plots shown are gated on leukocytes using side and forward scatter. Representative result of two independent experiments are shown. n = 3–5 per group.

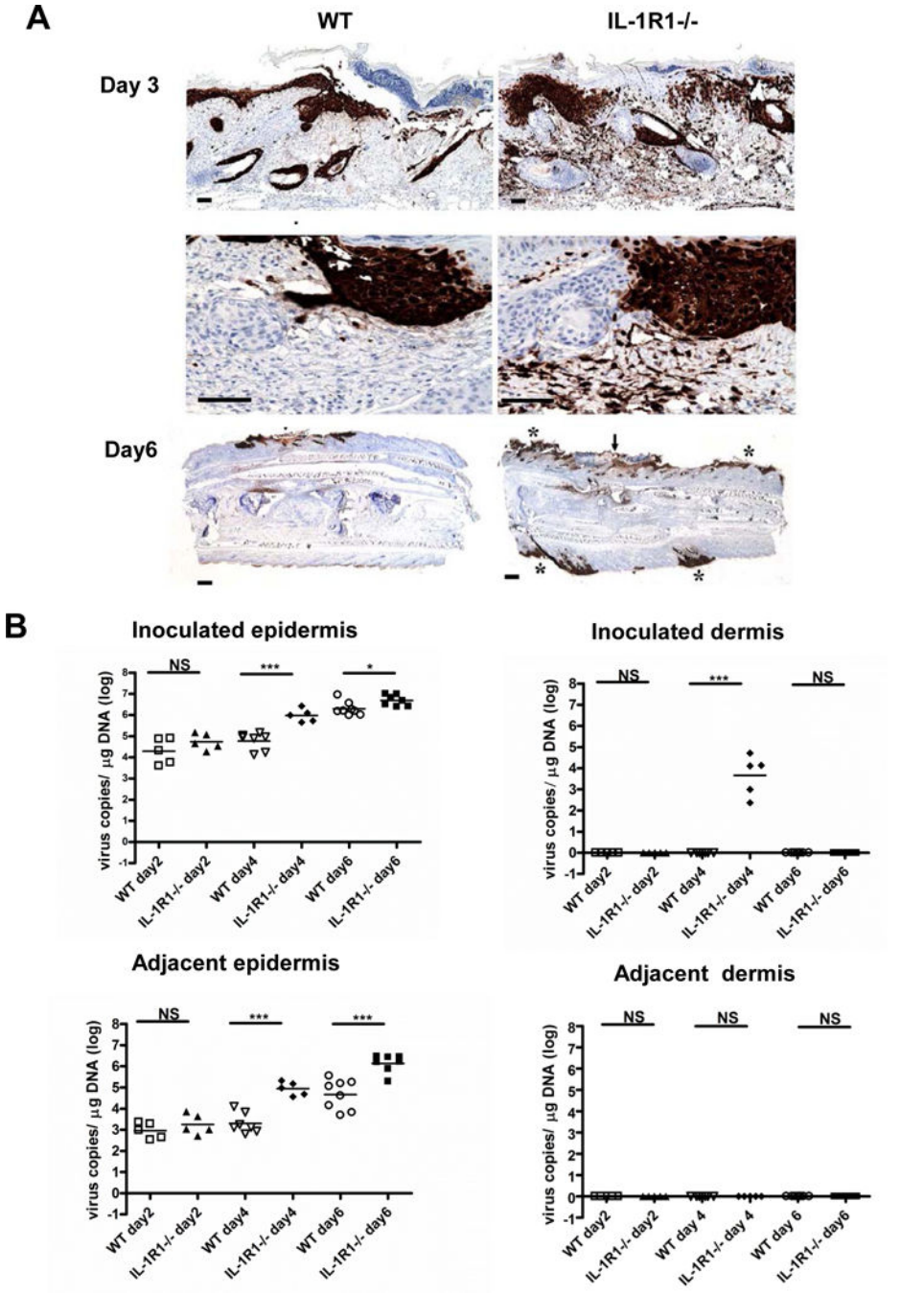

Figure 4. Lack of IL-1R1 facilitated VACV infection and replication in the epidermis and dermis *in vivo*

(A) 5×10^6 GFP-VACV was applied to IL-1R1−/− and WT mice by scarification. Anti-GFP Ab staining was used to identify VACV- infected cells (brown) at day 3 and day 6. Bars: Day 3: bars = 200 µm. Day 6: bars = 800µm. (B) Inoculated and adjacent skin were separated into epidermal and dermal layers at indicated time points following VACV scarification and VACV copy number per µg DNA was determined by quantitative PCR. Error bars represent mean ± SEM. n = 5–9 per group. * $P < 0.05$, ** $P < 0.01$, *** $P < 0.001$, NS = not significant.

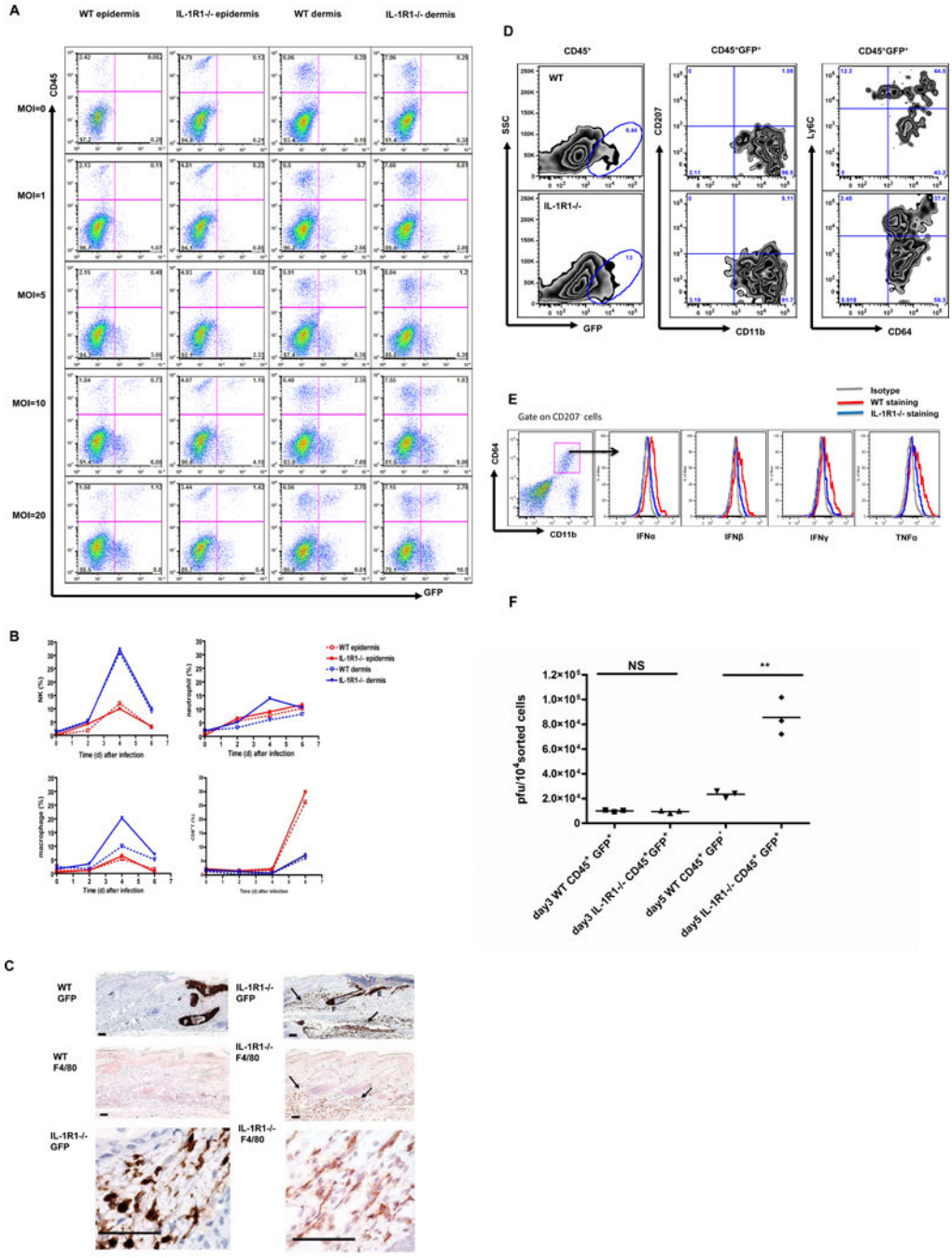

Figure 5. Deficiency of IL-1R1 did not influence infection of primary skin cells *in vitro*, but facilitated recruitment of macrophage-like cells in the dermis of VACV- scarified mice *in vivo*

(A) Primary epidermal and dermal cells were prepared from the skin of naïve IL-1R1−/− and WT mice. Cells (1×10^6) were infected with GFP-VACV at MOI from 1 to 20 for 6h. Viral infection was monitored by the expression of GFP using flow cytometry. (B) 5×10^6 pfu of WR-VACV was applied to IL-1R1−/− and WT mice by scarification. Epidermal and dermal cells were prepared at indicated time points. The percentage of NK cell, neutrophils, macrophages and CD8+ T cells was measured by flow cytometry. Representative results of two independent experiments are shown. n= 3–5 per group. (C) 5×10^6 GFP-VACV was

applied to IL-1R1−/− and WT mice by scarification. Anti-GFP Ab staining (dark brown) and anti-F4/80 (red brown) staining were used to characterize VACV infected cells at day 3. bar = 200 μm. (D) 5×10^6 GFP-VACV was applied to IL-1R1−/− and WT mice by scarification. Single cell suspension were prepared from inoculated skin. $CD45^+GFP^+$ leukocytes were analyzed for the expression of CD11b, CD207, CD64 and Ly6C. Representative results of two independent experiments are shown. n = 3–5 per group. (E) 5×10^6 WR-VACV was applied to IL-1R1−/− and WT mice by scarification. The $CD11b^+CD64^+$ $CD207^-$ cells from inoculated skin were analyzed for the expression of various cytokines. Representative results of two independent experiments are shown. n = 5 per group. (F) Viral titers (PFU) from sorted GFP^+ $CD45^+$ cells at day 3 and day 5 after VACV scarification were measured. This experiment was repeated 3 times, n = 5–7 per group. **P < 0.01, NS = not significant.

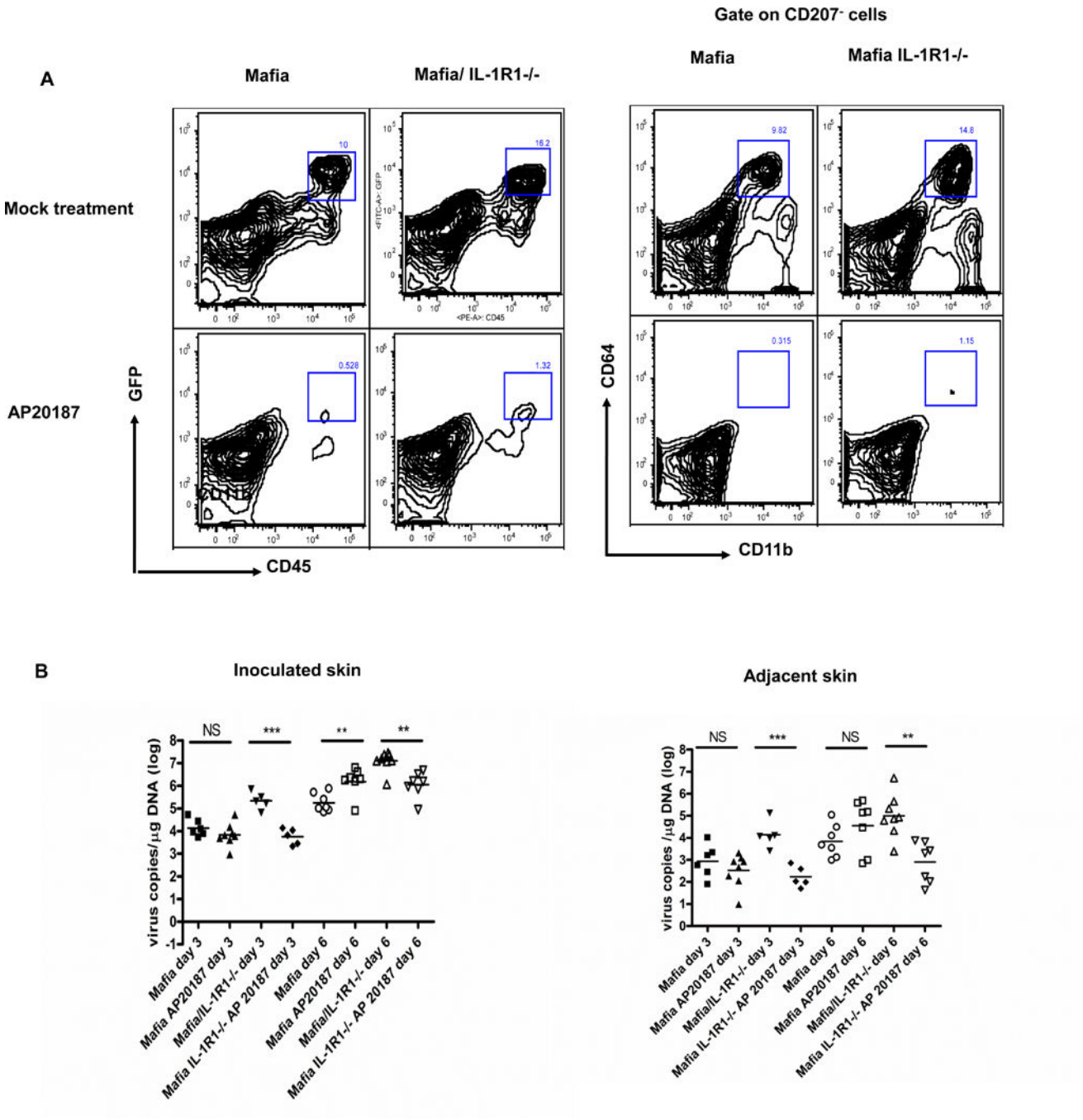

Figure 6. Conditional macrophage ablation reduced viral genome copies in VACV scarified skin of Mafia/IL-1R1−/− mice

Mafia and Mafia/IL-1R1−/− mice were scarified with 5×10^6 WR-VACV and treated with diluents (Mock treatment) or AP20187 (10mg/ml) for 5 days followed by AP20187 (1mg/ml) every 3 days. (A) Cells from VACV inoculated skin were analyzed for CD45 and GFP expression (left). $CD207^-$ cells from the VACV inoculated skin were gated for CD11b and CD64 expression (right). (B) Mafia and Mafia/IL-1R1−/− mice treated with diluent or AP20187 were sacrificed at day 3 and day 6. Inoculated skin and adjacent skin were

harvested for measurement of VACV copy number per μg DNA. Error bars represent mean ± SEM. n = 5–8 per group. * P < 0.05, ** P < 0.01, *** P< 0.001, NS = not significant.